Differential Effects of HIF2α Antagonist and HIF2α Silencing in Renal Cancer and Sensitivity to Repurposed Drugs

Esther Arnaiz
Department of Medical Oncology, Molecular Oncology Laboratories, Weatherall Institute of Molecular Medicine, University of Oxford, John Radcliffe Hospital, Oxford, OX3 9DS

Ana Miar (anbelen_mc@hotmail.com)
Department of Oncology, Old Road Campus Research Building, University of Oxford, Oxford, OX3 7DQ

Esther Bridges
Department of Medical Oncology, Molecular Oncology Laboratories, Weatherall Institute of Molecular Medicine, University of Oxford, John Radcliffe Hospital, Oxford, OX3 9DS

Naveen Prasad
Department of Oncology, Old Road Campus Research Building, University of Oxford, Oxford, OX3 7DQ

Stephanie B. Hatch
Nuffield Department of Medicine, NDM Research Building, University of Oxford, Oxford, OX3 7DQ, UK

Daniel Ebner
Nuffield Department of Medicine, NDM Research Building, University of Oxford, Oxford, OX3 7DQ, UK

Charles H. Lawrie
Department of Oncology, Molecular Oncology Group, Biodonostia Health Research Institute, Paseo Doctor Begiristain s/n San-Sebastián, 20014, Spain

Adrian L. Harris
Department of Medical Oncology, Molecular Oncology Laboratories, Weatherall Institute of Molecular Medicine, University of Oxford, John Radcliffe Hospital, Oxford, OX3 9DS

Research Article

Keywords: HIF2α, renal cancer, EMT, drug resistance.

Posted Date: February 25th, 2021

DOI: https://doi.org/10.21203/rs.3.rs-237320/v1

Version of Record: A version of this preprint was published at BMC Cancer on August 5th, 2021. See the published version at https://doi.org/10.1186/s12885-021-08616-8.

Abstract

Background: in clear cell renal cell carcinoma, 80% of cases have biallelic inactivation of the *VHL* gene, leading to constitutive activation of both HIF1α and HIF2α. As HIF2α is the driver of the disease promoting tumour growth and metastasis, drugs targeting HIF2α have been developed. However, resistance is common, therefore new therapies are needed.

Methods: we assessed the effect of the HIF2α antagonist PT2385 in several steps of tumour development and performed RNAseq to identify genes differentially expressed upon treatment. A drug screening was used to identify drugs with antiproliferative effects on *VHL*-mutated HIF2α-expressing cells and could increase effectiveness of PT2385.

Results: PT2385 did not reduce cell proliferation or clonogenicity but, in contrast to the genetic silencing of HIF2α, it reduced *in vitro* cell invasion. Many HIF-inducible genes were down-regulated upon PT2385 treatment, whereas some genes involved in cell migration or extracellular matrix were up-regulated. HIF2α was associated with resistance to statins, addition to PT2385 did not increase the sensitivity.

Conclusions: this study shows key differences between inhibiting a target versus knockdown, which are potentially targetable.

Background

Renal cell carcinoma (RCC) is amongst the 10 most common cancers[1]. The most common subtype of RCC is clear cell RCC (ccRCC, 70–85% of cases), characterised by high vascularity and showing lipid and glycogen accumulation in the cytoplasm[2]. Most ccRCC cases present biallelic inactivation of the von Hippel Lindau (*VHL*) tumour suppressor gene. Under normal oxygen conditions, VHL polyubiquitinates hypoxia-inducible factor 1 alpha (HIF1α) and 2 alpha (HIF2α) targeting them for proteasomal degradation, but in the absence of VHL, HIFα subunits can translocate to the nucleus, dimerize with HIF1β and transactivate the expression of their downstream genes[3]. Both HIF1α and HIF2α appear to be involved in ccRCC initiation, however, they have contrasting roles as the disease develops[4]. In contrast to other cancers, in ccRCC HIF1α functions as a tumour suppressor by attenuating tumour cell growth, whereas HIF2α promotes tumour development[4, 5]. Additionally, HIF pathway deregulation due to *VHL* mutation leads to ccRCC angiogenesis, and therefore, to the characteristic high vasculature of this tumour type[6]. Similarly, HIFs regulate every step of the metastatic process: from cell acquisition of motile and invasive phenotype (epithelial to mesenchymal transition, EMT), to inhibition of anoikis and later establishment of the premetastatic site prior to clonal expansion[7, 8]. Epigenetic alterations such as DNA methylation can regulate HIF2α-induced expression of metastatic genes in ccRCC[9], and superenhancer formation in inflammatory ccRCC cells promotes neutrophil-dependent lung metastasis[10]. Overall, HIF2α promotes metastasis in RCC[11, 12], and high HIF2α mRNA and protein expression in tumour tissue is associated with shorter survival[13].

Due to HIF2α involvement in ccRCC progression, drugs targeting HIF2α have recently been developed. Scheuermann *et al.* showed that small-molecule ligands such as PT2385, PT2399 and PT2977 can bind to a large hydrophobic cavity in the PAS-B domain of HIF2α, induce a conformational change, avoid the heterodimerization with HIF1β and finally impair the activation of downstream target gene expression[14–16]. PT2385 treatment inhibited the expression of HIF2α target genes in ccRCC cell lines and tumour xenografts and it promoted tumour regression faster than sunitinib[17], as did PT2399[18]. Moreover, a phase I trial in previously treated patients showed that PT2385 was well tolerated and that there were no dose limiting toxicities[19]. PT2399 was demonstrated to reduce lung metastasis in animal models *in vivo*[20]. These promising results promoted the development of the second-generation HIF2α antagonist PT2977 with the aim of improving PT2385's variable and dose-limited pharmacokinetics[21].

Nevertheless, long term exposure to these HIF2α inhibitors generates resistance via mutations in the HIF2α binding pocket or in the heterodimerization partner HIF1β[18, 22]. Therefore, it is necessary to use a different approach to discover drugs against this malignancy. Statins (small-molecule inhibitors of the 3-hydroxy-3-methyl-glutaryl-coenzyme A (HMG-CoA) reductase (HMGR), the rate limiting enzyme of the mevalonate pathway) are reported to be differentially toxic for VHL-defective ccRCC cell lines[23], suggesting that repurposing well-known and well-characterized drugs could provide a novel therapeutic strategy to target ccRCC combined with PT2385, as statins have long been used to reduce cholesterol levels[24].

We investigated the effects of PT2385 in ccRCC by analysing migration, invasion, the clonogenic potential and the alteration in gene expression. In addition, we evaluated the effect of the drugs in the Pharmakon 1600 library to identify currently used or approved drugs with possible additive effects in the treatment of ccRCC.

Methods

Cell culture and cell transfection

Both 786-0 cells (obtained from the American Type Culture Collection (ATCC®), CRL-1932™) and RCC4 cells, gift from W. Kaelin[25], were cultured in DMEM low glucose medium (1g/L) supplemented with 10% FBS no longer than 20 passages. They were mycoplasma tested every 3 months and all of them were authenticated using DNA STR analysis. 786-0 wild type (786-0 WT) cell line is *VHL* defective and contains an inactivating mutation in *HIF1α* gene, leading to constitutive expression of HIF2α. RCC4 *VHL* mutant cell line stably expressing an empty vector (RCC4 WT) or a vector for VHL overexpression (RCC4 VHL) were used.

Transfection of HIF2α siRNA (siHIF2α) and siRNA control (siCON) (Supplementary table 1) was performed with 12000 cells using Optimem reduced serum medium at a final concentration of 20nM. Oligofectamine (12252-011, Thermo Fisher) was used following the manufacturer's instructions.

Western blot

Cells were washed with cold PBS and lysed 30 min on ice with RIPA lysis buffer (R0278, Sigma) containing protease (cOmplete, 11697498001, Roche) and phosphatase (phosSTOP, 4906845001, Sigma) inhibitor cocktails. Lysates were cleared by centrifugation and supernatants were boiled at 95°C for 5 min in 4x NuPAGE LDS sample buffer (NP0007, Invitrogen) containing 10% β-mercaptoethanol. Samples were run on NuPAGE Novex 4–12% Bis-TRIS gels (NP0336BOX, Invitrogen) using NuPAGE MOPS-SDS running buffer (NP000102, Invitrogen). After transferring the proteins onto PVDF membranes (IPVH00010, Millipore), these were blocked with 5% milk (A0830,100, Applichem) in TBS-T (TBS containing 0.1% Tween-20) for 1h at room temperature and were then incubated overnight with anti-HIF2α primary antibody (NB100-122, Novus Biologicals) or β-actin peroxidase (A3854, Sigma) in 5% milk TBS-T at 4°C. Membranes were washed 3x in TBS-T and incubated with HRP-antirabbit secondary antibody (P0448, Agilent). Development was performed with Amersham ECL Prime Western Blotting Detection Reagent (GERPN2232, Sigma) using ImageQuant™ LAS 4000.

RT-qPCR

RNA was extracted using the Tri-Reagent protocol (T9424, Sigma) and 1µg of RNA was reverse transcribed into cDNA with the High Capacity cDNA reverse transcription kit (44368813, Thermo Fisher) using random hexamer primers. The PCR reaction containing SensiMix™ SYBR Green→ No-ROX Kit (QT650-20, Bioline) was run on a 7900 Real time PCR System with standard cycling conditions: 10 min 95°C, and 40 cycles of 15s 95°C followed by 1 min 60°C. Gene expression was analysed with the Ct method using *HPRT1* expression for normalization[26]. The primers used are listed in Supplementary table 2.

Migration assay

$1.2x10^4$ 786-0 cells or $2x10^4$ RCC4 cells were seeded per well in 96-well ImageLock™ plates (4379, Essen BioScience) and incubated for 24h. When the effect of PT2385 (B1920, BioVision) was tested, the compound was added to the wells once the cells were attached. After wounding, cells were washed with fresh media and plates were placed into the IncuCyte ZOOM→ until wound closure. Scanning was performed using a 10x objective and scheduled every 2h. Migration ability of the cells was analysed through two integrated metrics that the IncuCyte™ Software calculates based on the processed images: wound width and wound confluence. Wound width represents the average distance (µm) between the leading edge of the population of migrating cells (scratch wound mask) within an image. Wound confluence determines the percentage of wound area that is occupied by cells, and it relies on the initial scratch wound mask to differentiate the wounded from the non-wounded region.

Invasion assay

96-well ImageLock™ plate wells were coated with a thin layer of Matrigel→ Growth Factor Reduced Basement Membrane Matrix (354230, Corning) and the plate was placed in a 37ºC incubator, 5% CO_2

overnight. Matrigel® was removed and, 1.2x10^4 786-0 cells or 2x10^4 RCC4 cells were seeded per well and incubated for 24h. PT2385 was added once the cells were attached. After performing the wound and washing the wells, 50µL Matrigel® (8mg/ml) was added. The plate was placed in the incubator for 30 min prior the addition of 100µL cell culture media containing PT2385 or not. The plate was then placed into the IncuCyte ZOOM® for 5 days. Scanning was performed using a 10x objective and scheduled every 4h. The invasion ability of the cells was analysed using the relative wound density (RWD), which represents the density of the wound region relative to the density of the cell region, relying on the initial scratch wound mask to differentiate between cell-occupied and cell-free regions of the image.

Cell proliferation assay

To validate the screening hits, simvastatin (S6196, Sigma), fluvastatin sodium hydrate (SML0038, Sigma) and terbinafine hydrochloride (T8826, Sigma) were added to the cell culture and cell viability was analysed 5 days later using CyQUANT™ Cell Proliferation Assay (C7026, Invitrogen) as per manufacturer's instructions.

CyQUANT™ Cell Proliferation Assay was also used to determine cell proliferation after PT2385 treatment.

Colony formation assay

1000 cells were plated in 100mm plates in 20mL media and cultured for 10 days. Media was removed and Coomassie blue solution (H_2O containing 50% methanol, 7% acetic acid glacial (A/0360/PB17, Thermo Fisher) and 0.1% Brilliant Blue R (B7920, Sigma)) was added to fix and stain the colonies for 2h. Then, Coomassie blue solution was recovered and plates were washed with tap water and allowed to dry overnight. Plates were scanned using UMAX MagicScan software. Colony count was manually performed using Fiji Image J Software.

RNA sequencing (RNAseq)

The sequencing reads were checked for their quality using *FastQC* and low quality reads were trimmed using *cutadapt*. The trimmed reads were aligned to the human genome using *STAR*. Number of reads per gene (gene counts) was calculated using *featureCount*. Human assembly release GRCh38 was used for alignment and gene counting.

Differentially expressed genes (padj cut off < 0.05) and enriched gene ontological terms on biological processes or cellular components between 786-0 WT and 786-0 WT cells treated with 10µM PT2385 for 48h were identified and compared using the R package -*DESeq2* and *ClusterProfiler*, respectively. In short, three replicates of the experimental set were compared against three replicates of control set after removal of genes with very low counts.

The top 50 most up-regulated and 50 most down-regulated genes upon PT2385 treatment were extracted from the gene expression matrix after removing gene duplicates and used to create the heatmap.

High throughput screening

300 786-0 WT cells per well were seeded in 384-well plates (GN781090, Sigma) using a Perkin Elmer FlexDrop reagent dispenser the day before treatment. The Pharmakon 1600 library (MicroSource Discovery Systems), including antibacterial, antidiabetic, antifungal, antihypertensive, anti-inflammatory, diuretic, histamine or neurotransmitter-related drugs, among others, was diluted and added to the cells using a Janus automated workstation (PerkinElmer) resulting in final concentrations of 10μM, 1μM and 0.1μM, in duplicate. After a 3-day incubation the growth media was replaced with phenol red-free complete media containing 10μg/mL resazurin. The plates were incubated at 37°C, 5% CO_2 for 2h and then fluorescence was read using an Envision plate reader (PerkinElmer). After background subtraction, the data from each plate was normalised by calculating Z-scores.

Statistical analysis

GraphPad Prism 5.0 statistical analysis software (GraphPad Software) was used. When analysing the influence of two different independent variables on one dependent variable, 2-way ANOVA was applied. When two means were compared, t-test was performed.

Results

PT2385 does not inhibit growth of ccRCC cells

The effect of the HIF2α analogue PT2385 was assessed in ccRCC cell proliferation and clonogenic survival. As previously reported[17], PT2385 did not alter 786-0 WT cell proliferation (Fig. 1A) nor colony formation (Fig. 1B). The RCC4 cell line was also analysed. RCC4 VHL cells (reconstituted with non-mutated *VHL*) generated more colonies than RCC4 WT cells (which express both HIF1α and HIF2α) and addition of PT2385 did not reduce the clonogenic potential of RCC4 WT cells (Fig. 1B), demonstrating that it is not toxic for the cells *in vitro.*

PT2385 treatment promotes tumour cell migration in vitro

The effect of PT2385 on 786-0 and RCC4 cell migration was analysed using the IncuCyte ZOOM→. Whereas PT2385 did not change 786-0 cell migration (Fig. 2A), it promoted the migration of RCC4 WT cells (Fig. 2B). The RCC4 VHL cell line migrated faster than RCC4 WT closing the wound 24h after making the scratch compared to the 48h needed by RCC4 WT cells (Fig. 2B). Interestingly, PT2385 addition to RCC4 WT cells promoted their migration generating an intermediate phenotype between RCC4 WT and RCC4 VHL cells (Fig. 2B). This suggests that in the RCC4 cell line, not only HIF2α but also HIF1α is repressing cell migration.

HIF2α inhibition suppresses cell invasion in vitro

The invasion ability of these cell lines was also evaluated using the IncuCyte ZOOM→. Addition of PT2385 impeded invasion of 786-0 WT cells in a concentration-dependent manner (Fig. 3A). Conversely,

neither RCC4 WT nor RCC4 VHL cells were able to invade through the Matrigel, and PT2385 treatment did not have any effect (Fig. 3B).

HIF2α silencing does not affect cell migration or invasion in vitro

786-0 WT cells were transfected with either siCON or siHIF2α and their migratory and invasion potential was analysed. Similarly to HIF2α inhibition using PT2385, suppression of HIF2α with siRNA did not alter the migratory ability of 786-0 WT cells (Supplementary Fig. 1A), but in contrast to the inhibitor, HIF2α silencing did not reduce their invasion potential (Supplementary Fig. 1A). To exclude a possible residual HIF2α effect in the observed phenotype of 786-0 WT siHIF2α cells, the expression of HIF2α and known HIF2α target genes was analysed every 24h until the end of the experiment. HIF2α was not induced over time (Supplementary Fig. 1B), and its downstream targets *GLUT1* and *VEGFA* were not consequently up-regulated (Supplementary Fig. 1C).

RNAseq comparison of the parental cell line with PT2385 effects

RNAseq showed that the most differentially expressed genes upon PT2385 treatment were related to renal development and hypoxia biological processes, followed by GO terms involved in cell migration, such as actin filament organization, tissue migration or regulation of cytoskeleton organization (Supplementary Fig. 2A). Supporting the enriched GO terms for biological processes, enriched GO terms for cellular components were related to cell migration/invasion and cell-cell or cell-extracellular matrix interaction (ECM) (Supplementary Fig. 2B).

Additionally, RNAseq analysis showed an expected down-regulation of many well documented HIF-induced genes upon PT2385 treatment (e.g. *NDRG1, SLC2A1, EGLN3* or *ROR2*) but several other genes were up-regulated (Fig. 4, see Supplementary table 3 for full names). This last group included genes involved in cell migration and ECM (e.g. *RAB6B*, *FN1, VCAM1* or *COL14A1*) and genes of signalling pathways usually deregulated in cancer, such as Notch and Wnt signalling (*JAG1* and *WNT7B*, respectively).

HIF2α confers resistance to statin treatment

The lack of toxicity of PT2385 but its effect on tumour cell movement led us to investigate if there were currently used drugs to which ccRCC cells would be sensitised.

The drug screening performed in 786-0 WT cells identified several lethal compounds (Fig. 5A). With the exception of a single plate, which was excluded from the analysis due to a plating error, the correlation between the replicates was good, with an average Pearson's coefficient of 0.920. Taking into account previously published data[23], the statins simvastatin and fluvastatin were further analysed, as well as the squalene monooxygenase inhibitor terbinafine, which blocks cholesterol synthesis while allows the synthesis of non-sterol isoprenoids. We showed that the resistance of 786-0 WT cells to statins was due to HIF2α expression, as silencing HIF2α made the cells more sensitive (Fig. 5B). Supporting the lack of

toxicity of PT2385, addition of this HIF2α analogue did not inhibit further 786-0 WT cell proliferation. However, HIF2α-expressing cells appeared to be more sensitive to terbinafine (Fig. 5B), and as for the statins, addition of PT2385 did not have any additional effect.

Discussion

Metastasis is a multistep process which selects for highly aggressive tumour cells, as they acquire the ability to disseminate from the primary tumour and grow at distant sites[27]. Here, we show that the oncoprotein HIF2α is involved in *in vitro* cell migration and invasion, as has already been described for many tumour cell lines[28–30].

Interestingly, HIF2α blockage had opposing effects depending on the agent used. Treatment with PT2385 did not affect 786-0 cell migration, while partially abolishing cell invasion in a concentration-dependent manner. However, silencing of HIF2α by siRNA did not change the migration or invasion ability of 786-0 cells. PT2385 allosterically binds to HIF2α and thereby prevents the heterodimerization with HIF1β and its subsequent binding to the DNA[31], whereas siRNA binds to complementary mRNA and targets them for degradation in a transitory manner[32]. HIF2α silencing was successfully achieved during the invasion experiment but at the endpoint (96h), HIF2α started to re-express. These results suggest that the few molecules escaping siRNA silencing might be enough to keep the phenotype, even though they are not detectable at protein level. On the other hand, PT2385 treatment showed that DNA binding is not completely abolished by the inhibitor, as previously reported[22], as cell invasion was not 100% suppressed.

Supporting HIF2α involvement in ccRCC migration, RCC4 VHL cells migrated more than RCC4 WT, in contrast to previous publications[33, 34]. In this case, as they also express HIF1α, both HIF2α and HIF1α could be inhibiting cell migration; however, treatment with PT2385 generated an intermediate phenotype pointing to a more important role of HIF2α.

RNAseq results showed the already known specificity of PT2385 for HIF2α. PT2385 treatment down-regulated the expression of genes involved in hypoxic response (*EGLN3* or *CA12*), migration (*SEMA6A/5B*) and metastasis (*ITGB8* or *VEGFA*). These results support the previously described effect of PT2385 avoiding ccRCC tumour progression and metastasis[17]. On the other hand, PT2385 treatment increased the expression of genes involved in cell-cell or cell-ECM interaction, such as *FN1, VCAM1, COL14A1* or *ADAMTS15.* High abundance of components of the ECM like fibronectin 1 or collagen can possibly explain the inhibition of PT2385 in cell invasion, as the cells might not be able to degrade the ECM and move through it. In addition, high levels of cell-cell adhesion molecules such as VCAM1 could also reduce cell movement.

However, the increased expression of genes upon PT2385 treatment suggests one way of enhancing the effect of PT2385 could be via combination therapy targeting those molecules. Fibronectin, for instance, exists in multiple isoforms and in adulthood the expression of EDA and EDB domains is very restricted in normal tissue, whereas it is highly expressed in tumours[35]. This has led to the development of drugs or

antibodies against these domains as a mechanism of delivering drugs to the tumour site[36, 37]. Treatment of PT2385 increases FN1 expression, increasing the amount of target fibronectin in the tumour and possibly making it easier to specifically deliver tumour-directed drugs. In addition, PT2385 increased the expression of JAG1, suggesting that the combination of Notch signalling inhibitors already used in clinic with PT2385 could be of benefit for renal cancer treatment. Bhagat *et al.* (2016) found that genetic and epigenetic alterations in ccRCC tissues led to both Notch ligand and receptor overexpression[38]. JAG1, for instance, was overexpressed and associated with loss of CpG methylation of HeK4me1-associated enhancer regions. They confirmed the procarcinogenic role of Notch *in vivo*, as previously reported[39], and showed that treatment with the gamma-secretase inhibitor LY3039478 avoided ccRCC cell growth both *in vitro* and *in vivo*.

Supporting previous observations that HIF2α silencing does not affect *in vitro* ccRCC growth under standard culture conditions[4, 40], addition of PT2385 did not inhibit tumour cell proliferation or colony formation at concentrations up to 10μM[17], and its combination with statins did not increase statin-driven inhibition of cell proliferation. But both the synthetic statin fluvastatin and the semi-synthetic statin simvastatin impaired proliferation in HIF2α knockdown cells. It has been described that statins inhibit ccRCC cell proliferation via targeting the mTOR pathway both *in vitro* and *in vivo*[41, 42]. mTOR is the target of Temsirolimus and Everolimus, drugs currently used for ccRCC treatment, therefore, statins could be considered as possible repurposed drugs for ccRCC. In addition, using the Library of Pharmacologically Active Compounds (LOPAC)[1280], statins were detected as potent inhibitors of lymphangiogesis *in vitro*[43].

Another approach for developing new therapy options in combination with PT2385 would be to identify target genes with synthetic lethal relationship with HIF2α silencing. Nicholson *et al.* identified CDK4 and CDK6 as genes with lethal relationship with *VHL* loss, as loss of either gene alone was well tolerated, but the concurrent loss of both was lethal[44]. Supporting our results, they found that both simvastatin and fluvastatin inhibited the growth of VHL-reconstituted 786-0 cells more substantially than their VHL-defective counterparts. However, in contrast to a previous study[23], our results showed that statin-induced lethality is not due to *VHL* loss and the consequent HIFs expression, but associated with HIF2α loss. Thus HIF2α-conferred protection against statins suggests that one way of repurposing these drugs could be via combination treatment with HIF2α antagonists. Although we were not able to detect differences in cell proliferation *in vitro*, previously published data on HIF2α antagonists showed *in vivo* effects[17, 18]. However, we are in agreement with Thompson *et al.*[23] suggesting that the key branch for the observed phenotype is the blockage of isoprenylation and not the cholesterol synthesis pathway, as the lethal effect could not be rescued after treatment with squalene[23] and 786-0 siHIF2α cells were not sensitive to terbinafine.

Conclusions

Our study shows new therapy avenues to build on PT2385, as some of the genes that are up-regulated by HIF2α inhibition, are potential targets for combination treatments.

Abbreviations

ATCC, American Type Culture Collection; RCC, renal cell carcinoma; ccRCC, clear cell renal cell carcinoma; VHL, Von Hippel-Lindau; HIF1α, hypoxia-inducible factor 1 alpha; HIF2α, hypoxia-inducible factor 2 alpha; ECM, extracellular matrix; EMT, epithelial to mesenchymal transition; HMG-CoA, 3-hydroxy-3-methyl-glutaryl-coenzyme A; HMGR, HMG-CoA reductase; RWD, relative wound density; padj, adjusted p-value; RNA sequencing, RNAseq.

Declarations

Ethics approval and consent to participate

Not applicable.

Consent for publication

Not applicable.

Availability of data and materials

The RNAseq data generated and analysed during the current study is available in the NCBI's Gene Expression Omnibus repository, and is accessible through GEO Series accession number GSE153711 (https://www.ncbi.nlm.nih.gov/geo/query/acc.cgi?acc=GSE153711).

Competing interests

The authors declare that they have no competing interests.

Funding

This work was supported by funding from Cancer Research UK and the Basque Country Government (PRE_2018_2_0018).

Author's contribution

E.A., A.M. and A.L.H. designed the experiments and wrote the manuscript. E.A. performed the experiments and analysed the data. N.P. analysed the RNAseq experiments. S.B.H. analysed the drug screening. D.E. designed the drug screening and reviewed the manuscript. C.H.L. and E.B. reviewed the manuscript.

Acknowledgements

Not applicable.

Authors' information

EA's present address: Cambridge Institute for Therapeutic Immunology & Infectious Disease, Jeffrey Cheah Biomedical Centre, Puddlecombe Way, Cambridge, CB2 0AW, UK.

EB's present address: Nuffield Department of Medicine, Weatherall Institute of Molecular Medicine, University of Oxford, John Radcliffe Hospital, Oxford, OX3 9DS, UK.

CHL's additional affiliations: 1) Radcliffe Department of Medicine, University of Oxford, John Radcliffe Hospital, Oxford, OX3 9DU, UK, 2) IKERBASQUE, Basque Foundation for Science, María Díaz Haroko Kalea 3, Bilbao, 48013, Spain.

References

1. Capitanio U, Bensalah K, Bex A, Boorjian SA, Bray F, Coleman J, et al. Epidemiology of Renal Cell Carcinoma. *European urology*. 2019;75(1):74–84.
2. Wettersten HI, Aboud OA, Lara PN, Jr., Weiss RH. Metabolic reprogramming in clear cell renal cell carcinoma. *Nature reviews Nephrology*. 2017;13(7):410–9.
3. Huang LE, Gu J, Schau M, Bunn HF. Regulation of hypoxia-inducible factor 1alpha is mediated by an O2-dependent degradation domain via the ubiquitin-proteasome pathway. *Proceedings of the National Academy of Sciences of the United States of America*. 1998;95(14):7987–92.
4. Raval RR, Lau KW, Tran MG, Sowter HM, Mandriota SJ, Li JL, et al. Contrasting properties of hypoxia-inducible factor 1 (HIF-1) and HIF-2 in von Hippel-Lindau-associated renal cell carcinoma. *Molecular and cellular biology*. 2005;25(13):5675–86.
5. Gordan JD, Lal P, Dondeti VR, Letrero R, Parekh KN, Oquendo CE, et al. HIF-alpha effects on c-Myc distinguish two subtypes of sporadic VHL-deficient clear cell renal carcinoma. *Cancer cell*. 2008;14(6):435–46.
6. Rey S, Semenza GL. Hypoxia-inducible factor-1-dependent mechanisms of vascularization and vascular remodelling. *Cardiovascular research*. 2010;86(2):236–42.
7. Gilkes DM, Semenza GL. Role of hypoxia-inducible factors in breast cancer metastasis. *Future oncology (London, England)*. 2013;9(11):1623–36.
8. Schito L, Rey S, Tafani M, Zhang H, Wong CC, Russo A, et al. Hypoxia-inducible factor 1-dependent expression of platelet-derived growth factor B promotes lymphatic metastasis of hypoxic breast cancer cells. *Proceedings of the National Academy of Sciences of the United States of America*. 2012;109(40):E2707-16.
9. Vanharanta S, Shu W, Brenet F, Hakimi AA, Heguy A, Viale A, et al. Epigenetic expansion of VHL-HIF signal output drives multiorgan metastasis in renal cancer. *Nature medicine*. 2013;19(1):50–6.
10. Nishida J, Momoi Y, Miyakuni K, Tamura Y, Takahashi K, Koinuma D, et al. Epigenetic remodelling shapes inflammatory renal cancer and neutrophil-dependent metastasis. *Nature cell biology*. 2020;22(4):465–75.

11. Rankin EB, Fuh KC, Castellini L, Viswanathan K, Finger EC, Diep AN, et al. Direct regulation of GAS6/AXL signaling by HIF promotes renal metastasis through SRC and MET. *Proceedings of the National Academy of Sciences of the United States of America*. 2014;111(37):13373–8.
12. Rodrigues P, Patel SA, Harewood L, Olan I, Vojtasova E, Syafruddin SE, et al. NF-kappaB-Dependent Lymphoid Enhancer Co-option Promotes Renal Carcinoma Metastasis. *Cancer discovery*. 2018;8(7):850–65.
13. Wierzbicki PM, Klacz J, Kotulak-Chrzaszcz A, Wronska A, Stanislawowski M, Rybarczyk A, et al. Prognostic significance of VHL, HIF1A, HIF2A, VEGFA and p53 expression in patients with clearcell renal cell carcinoma treated with sunitinib as firstline treatment. *International journal of oncology*. 2019;55(2):371–90.
14. Key J, Scheuermann TH, Anderson PC, Daggett V, Gardner KH. Principles of ligand binding within a completely buried cavity in HIF2alpha PAS-B. *Journal of the American Chemical Society*. 2009;131(48):17647–54.
15. Rogers JL, Bayeh L, Scheuermann TH, Longgood J, Key J, Naidoo J, et al. Development of inhibitors of the PAS-B domain of the HIF-2alpha transcription factor. *Journal of medicinal chemistry*. 2013;56(4):1739–47.
16. Scheuermann TH, Tomchick DR, Machius M, Guo Y, Bruick RK, Gardner KH. Artificial ligand binding within the HIF2alpha PAS-B domain of the HIF2 transcription factor. *Proceedings of the National Academy of Sciences of the United States of America*. 2009;106(2):450–5.
17. Wallace EM, Rizzi JP, Han G, Wehn PM, Cao Z, Du X, et al. A Small-Molecule Antagonist of HIF2alpha Is Efficacious in Preclinical Models of Renal Cell Carcinoma. *Cancer research*. 2016;76(18):5491–500.
18. Chen W, Hill H, Christie A, Kim MS, Holloman E, Pavia-Jimenez A, et al. Targeting renal cell carcinoma with a HIF-2 antagonist. *Nature*. 2016;539(7627):112–7.
19. Courtney KD, Infante JR, Lam ET, Figlin RA, Rini BI, Brugarolas J, et al. Phase I Dose-Escalation Trial of PT2385, a First-in-Class Hypoxia-Inducible Factor-2α Antagonist in Patients With Previously Treated Advanced Clear Cell Renal Cell Carcinoma. *Journal of Clinical Oncology*. 2018;36(9):867–74.
20. Cho H, Kaelin WG. Targeting HIF2 in Clear Cell Renal Cell Carcinoma. *Cold Spring Harbor symposia on quantitative biology*. 2016;81:113–21.
21. Xu R, Wang K, Rizzi JP, Huang H, Grina JA, Schlachter ST, et al. 3-[(1S,2S,3R)-2,3-Difluoro-1-hydroxy-7-methylsulfonylindan-4-yl]oxy-5-fluorobenzo nitrile (PT2977), a Hypoxia-Inducible Factor 2alpha (HIF-2alpha) Inhibitor for the Treatment of Clear Cell Renal Cell Carcinoma. *Journal of medicinal chemistry*. 2019;62(15):6876–93.
22. Wu D, Su X, Lu J, Li S, Hood BL, Vasile S, et al. Bidirectional modulation of HIF-2 activity through chemical ligands. *Nature chemical biology*. 2019;15(4):367–76.
23. Thompson JM, Alvarez A, Singha MK, Pavesic MW, Nguyen QH, Nelson LJ, et al. Targeting the Mevalonate Pathway Suppresses VHL-Deficient CC-RCC through an HIF-Dependent Mechanism. *Molecular cancer therapeutics*. 2018;17(8):1781–92.

24. Shepherd J, Cobbe SM, Ford I, Isles CG, Lorimer AR, MacFarlane PW, et al. Prevention of coronary heart disease with pravastatin in men with hypercholesterolemia. 1995. *Atherosclerosis Supplements*. 2004;5(3):91 – 7.
25. Iliopoulos O, Kibel A, Gray S, Kaelin WG, Jr. Tumour suppression by the human von Hippel-Lindau gene product. *Nature medicine*. 1995;1(8):822–6.
26. Miar A, Arnaiz E, Bridges E, Beedie S, Cribbs AP, Downes DJ, et al. Hypoxia induces transcriptional and translational downregulation of the type I interferon (IFN) pathway in multiple cancer cell types. *bioRxiv*. 2019:715151.
27. Rankin EB, Giaccia AJ. Hypoxic control of metastasis. *Science (New York, NY)*. 2016;352(6282):175–80.
28. Wang Y, Li Z, Zhang H, Jin H, Sun L, Dong H, et al. HIF-1alpha and HIF-2alpha correlate with migration and invasion in gastric cancer. *Cancer biology & therapy*. 2010;10(4):376–82.
29. Wang X, Schneider A. HIF-2alpha-mediated activation of the epidermal growth factor receptor potentiates head and neck cancer cell migration in response to hypoxia. *Carcinogenesis*. 2010;31(7):1202–10.
30. Torres A, Erices JI, Sanchez F, Ehrenfeld P, Turchi L, Virolle T, et al. Extracellular adenosine promotes cell migration/invasion of Glioblastoma Stem-like Cells through A3 Adenosine Receptor activation under hypoxia. *Cancer letters*. 2019;446:112–22.
31. Scheuermann TH, Li Q, Ma HW, Key J, Zhang L, Chen R, et al. Allosteric inhibition of hypoxia inducible factor-2 with small molecules. *Nature chemical biology*. 2013;9(4):271–6.
32. Dana H, Chalbatani GM, Mahmoodzadeh H, Karimloo R, Rezaiean O, Moradzadeh A, et al. Molecular Mechanisms and Biological Functions of siRNA. *International journal of biomedical science: IJBS*. 2017;13(2):48–57.
33. Hu H, Takano N, Xiang L, Gilkes DM, Luo W, Semenza GL. Hypoxia-inducible factors enhance glutamate signaling in cancer cells. *Oncotarget*. 2014;5(19):8853–68.
34. Sumi C, Matsuo Y, Kusunoki M, Shoji T, Uba T, Iwai T, et al. Cancerous phenotypes associated with hypoxia-inducible factors are not influenced by the volatile anesthetic isoflurane in renal cell carcinoma. *PloS one*. 2019;14(4):e0215072.
35. Kumra H, Reinhardt DP. Fibronectin-targeted drug delivery in cancer. *Advanced drug delivery reviews*. 2016;97:101–10.
36. Frey K, Schliemann C, Schwager K, Giavazzi R, Johannsen M, Neri D. The Immunocytokine F8-IL2 Improves the Therapeutic Performance of Sunitinib in a Mouse Model of Renal Cell Carcinoma. *The Journal of Urology*. 2010;184(6):2540–8.
37. Johannsen M, Spitaleri G, Curigliano G, Roigas J, Weikert S, Kempkensteffen C, et al. The tumour-targeting human L19-IL2 immunocytokine: Preclinical safety studies, phase I clinical trial in patients with solid tumours and expansion into patients with advanced renal cell carcinoma. *European Journal of Cancer*. 2010;46(16):2926–35.

38. Bhagat TD, Zou Y, Huang S, Park J, Palmer MB, Hu C, et al. Notch Pathway Is Activated via Genetic and Epigenetic Alterations and Is a Therapeutic Target in Clear Cell Renal Cancer. *The Journal of biological chemistry*. 2017;292(3):837–46.
39. Sjölund J, Johansson M, Manna S, Norin C, Pietras A, Beckman S, et al. Suppression of renal cell carcinoma growth by inhibition of Notch signaling in vitro and in vivo. *The Journal of clinical investigation*. 2008;118(1):217–28.
40. Cho H, Du X, Rizzi JP, Liberzon E, Chakraborty AA, Gao W, et al. On-target efficacy of a HIF-2alpha antagonist in preclinical kidney cancer models. *Nature*. 2016;539(7627):107–11.
41. Woodard J, Sassano A, Hay N, Platanias LC. Statin-dependent suppression of the Akt/mammalian target of rapamycin signaling cascade and programmed cell death 4 up-regulation in renal cell carcinoma. *Clinical cancer research: an official journal of the American Association for Cancer Research*. 2008;14(14):4640–9.
42. Fang Z, Tang Y, Fang J, Zhou Z, Xing Z, Guo Z, et al. Simvastatin inhibits renal cancer cell growth and metastasis via AKT/mTOR, ERK and JAK2/STAT3 pathway. *PloS one*. 2013;8(5):e62823.
43. Schulz MMP, Reisen F, Zgraggen S, Fischer S, Yuen D, Kang GJ, et al. Phenotype-based high-content chemical library screening identifies statins as inhibitors of in vivo lymphangiogenesis. *Proceedings of the National Academy of Sciences*. 2012;109(40):E2665-E74.
44. Nicholson HE, Tariq Z, Housden BE, Jennings RB, Stransky LA, Perrimon N, et al. HIF-independent synthetic lethality between CDK4/6 inhibition and VHL loss across species. *Science signaling*. 2019;12(601):eaay0482.

Figures

Figure 1

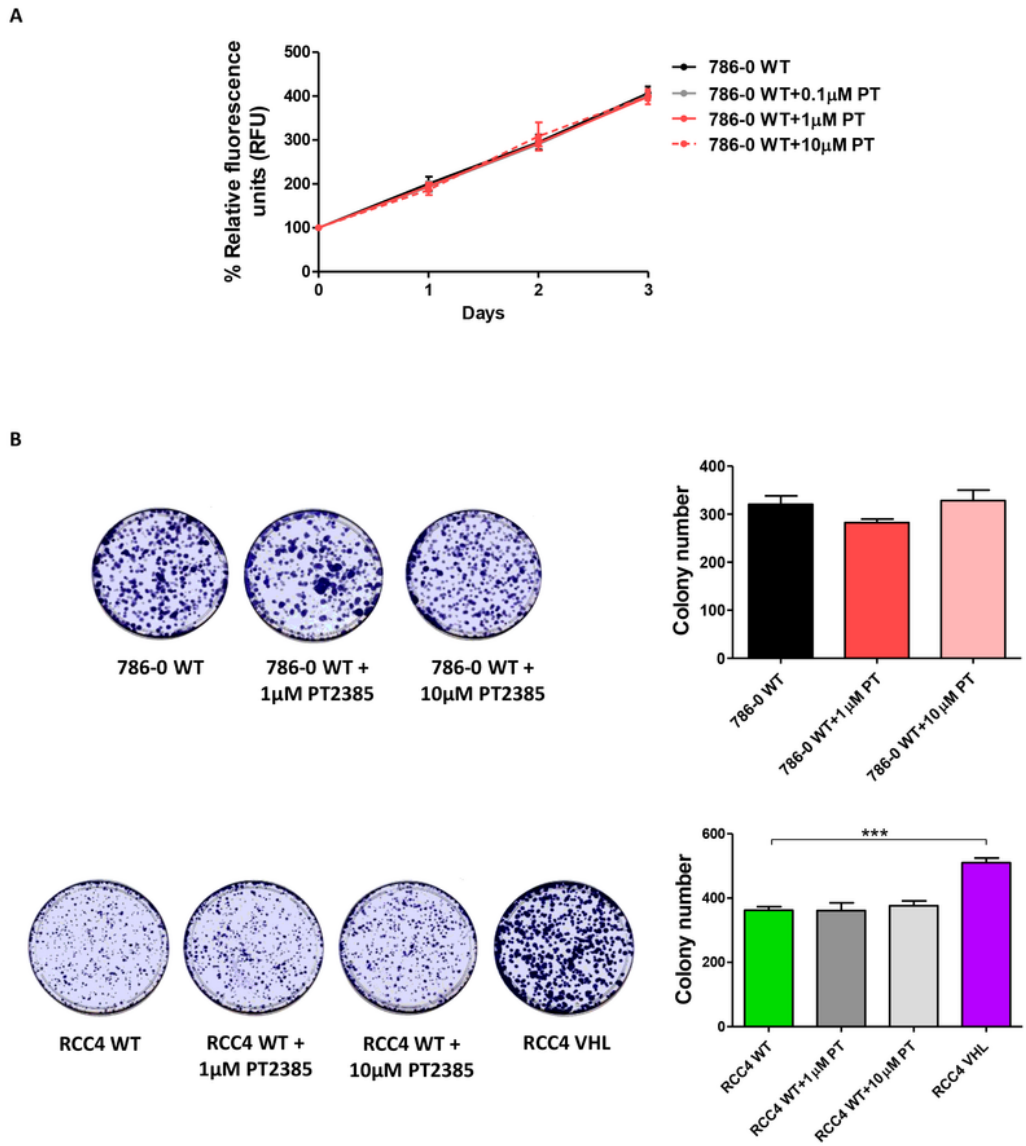

Figure 1

PT2385 effect on cell proliferation and clonogenic survival. A) 786-0 WT cell proliferation during four days after the addition of 0.1μM, 1μM or 10μM PT2385 (PT) relative to cells treated with DMSO. n=3. B) Representative images of 786-0 and RCC4 clonogenic assays and colony count. n=3. * $p<0.05$, ** $p<0.01$, *** $p<0.001$. Errors bars depict standard error of the mean.

Figure 2

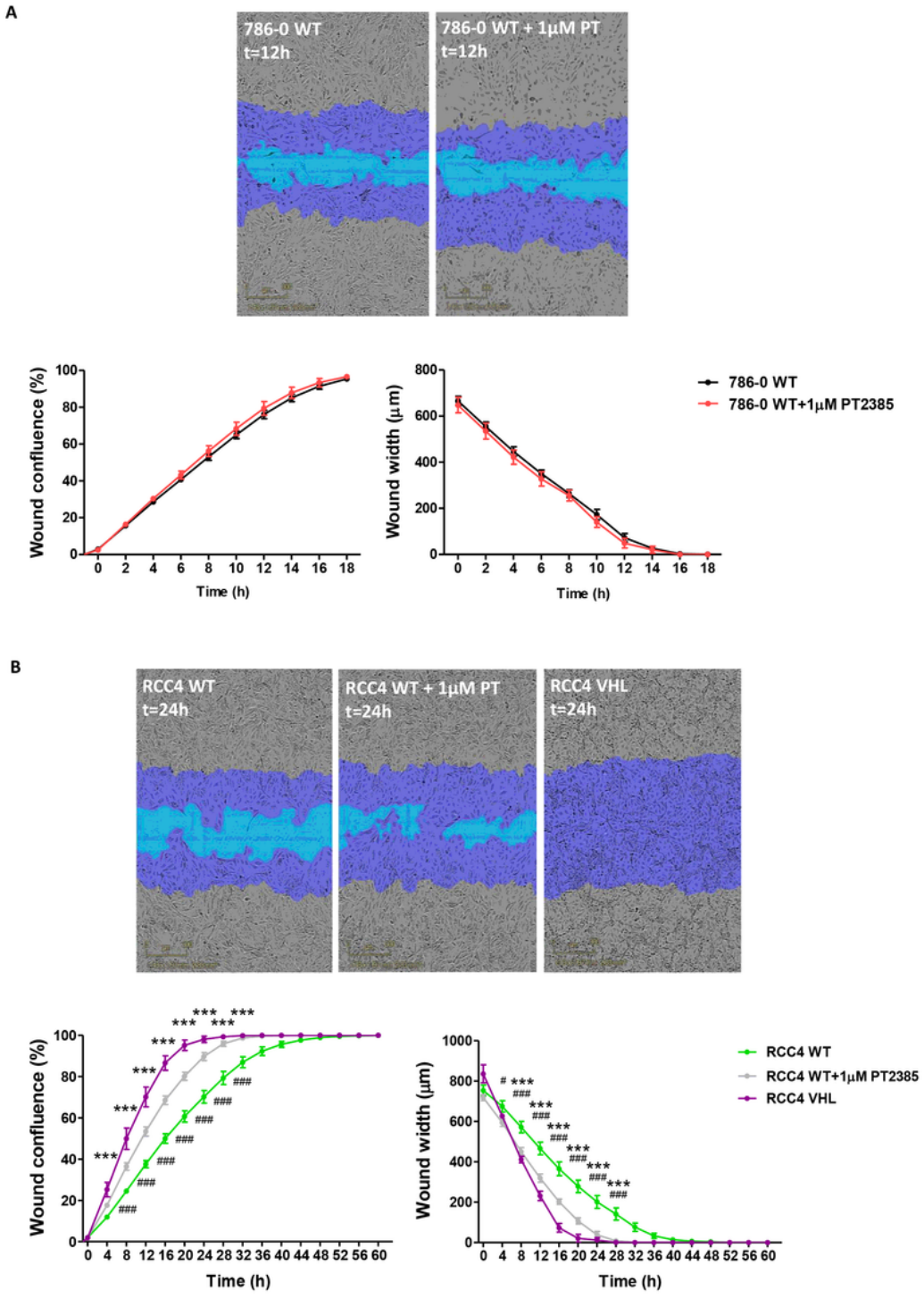

Figure 2

786-0 and RCC4 cell migration. A) Representative images of 786-0 WT and 786-0 WT+1µM PT2385 (PT) cells migrating 12h after the scratch and wound confluence and wound width measure until the complete closure of the wound. n=3. B) Representative images of RCC4 WT, RCC4 WT+1µM PT2385 (PT) and RCC4 VHL cells migrating 24h after the scratch and wound confluence and wound width measure until the complete closure of the wound. n=3. * represents comparison between RCC4 WT and RCC4 VHL and

represents comparison between RCC4 WT and RCC4 WT+1μM PT2385. Purple region corresponds to the initial scratch mask, whereas blue region represents the wound lacking cells at the compared moment. * p<0.05, ** p<0.01, *** p<0.001. Errors bars depict standard error of the mean.

Figure 3

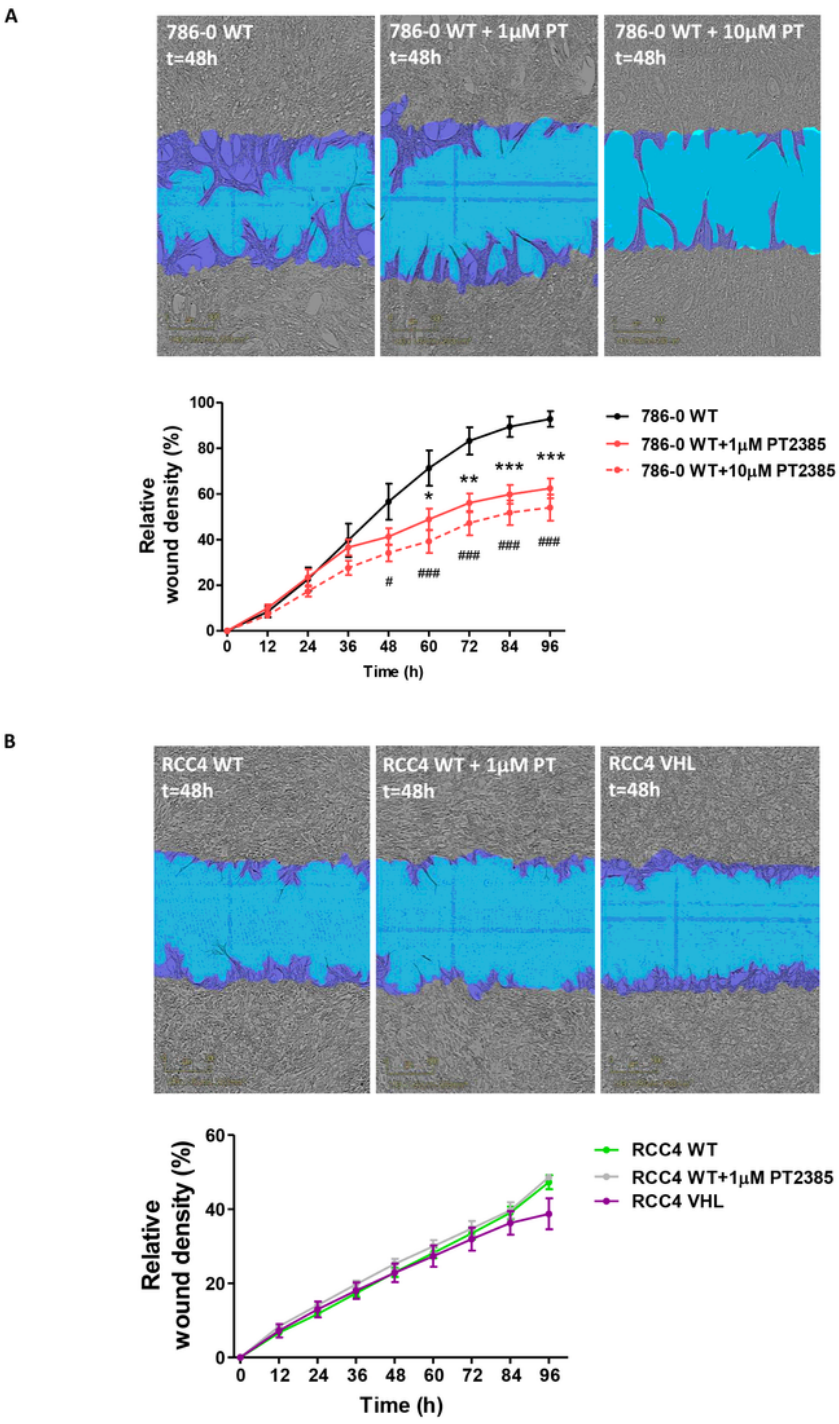

Figure 3

786-0 and RCC4 cell invasion. A) Representative images of 786-0 WT and 786-0 WT+1/10μM PT2385 (PT) cells invading 48h after the scratch and RWD measurement until 96h after wound performing. n=3. *

represents comparison between 786-0 WT and 786-0 WT+1μM PT2385 and # represents comparison between 786-0 WT and 786-0 WT+10μM PT2385. B) Representative images of RCC4 WT, RCC4 WT+1μM PT2385 (PT) and RCC4 VHL cells invading the wound 48h after the scratch and RWD measurement until 96h after wound performing. Purple region corresponds to the initial scratch mask, whereas blue region represents the wound lacking cells at the compared moment. n=3. * p<0.05, ** p<0.01, *** p<0.001. Errors bars depict standard error of the mean.

Figure 4

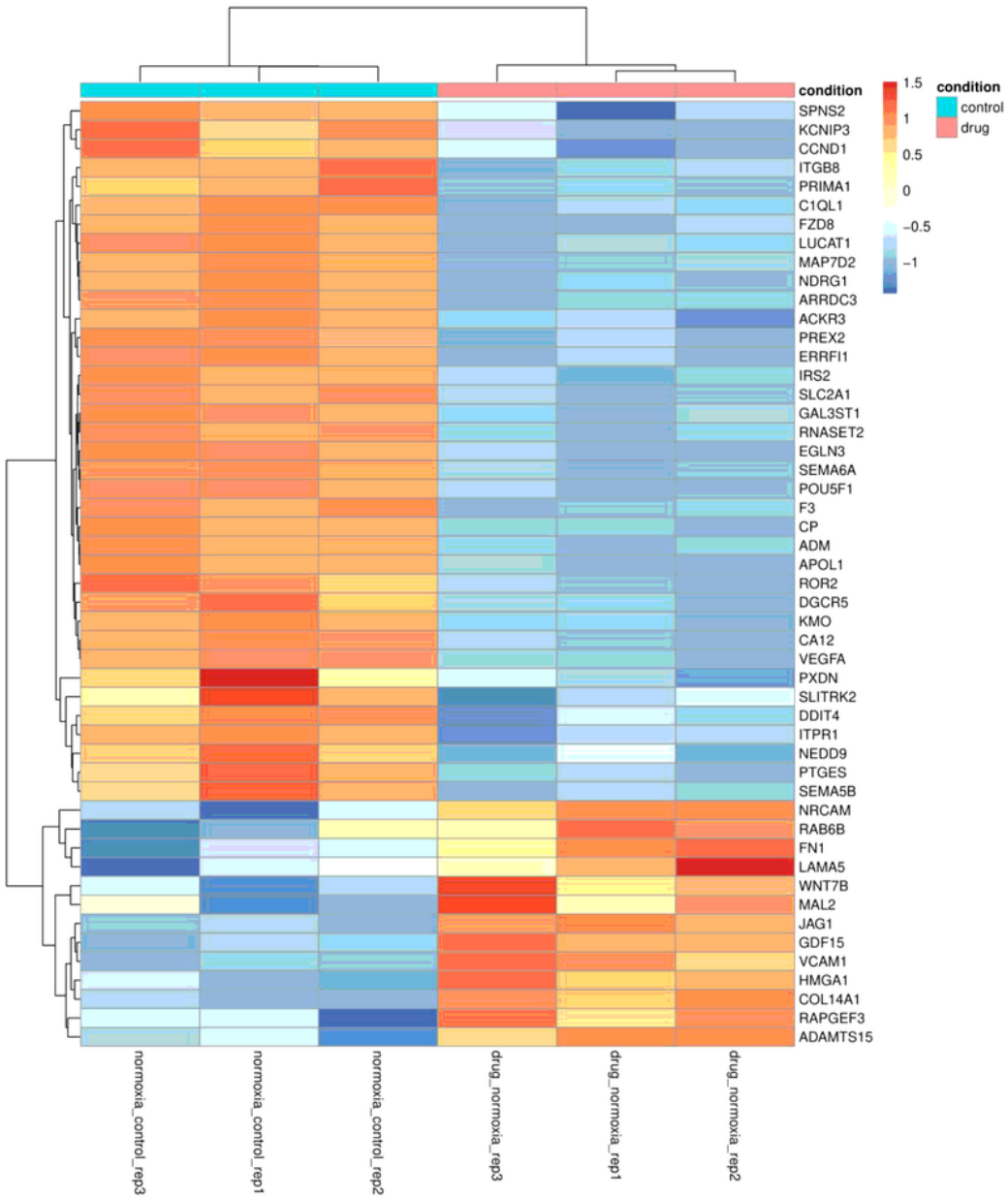

Figure 4

RNAseq results. Heatmap of the top 50 variant significant genes in 786-0 WT cells vs PT2385 treatment.

Figure 5

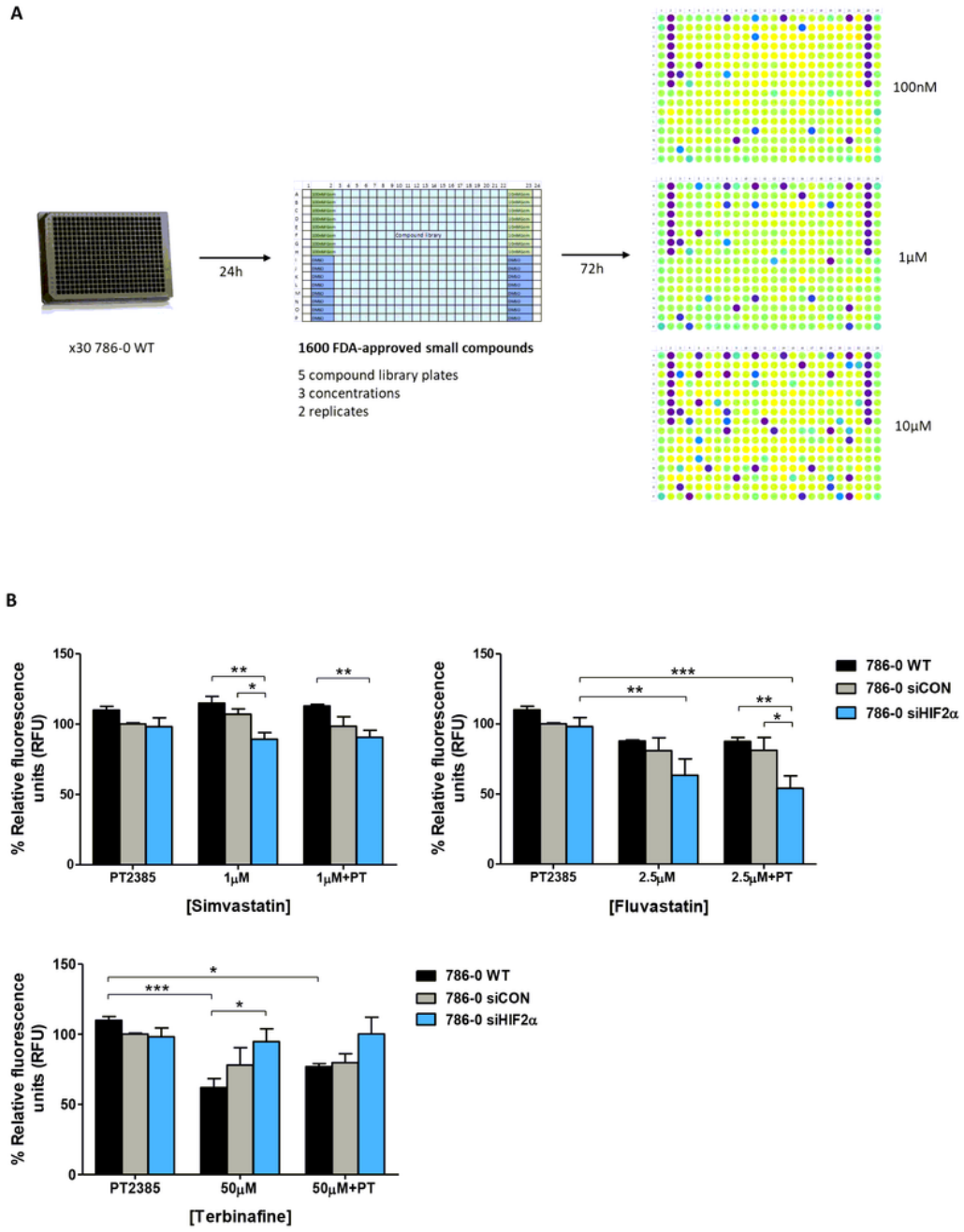

Figure 5

Drug screening of 786-0 WT cells. A) Diagram showing the drug screening. B) Viability of 786-0 WT and 786-0 WT cells transfected with siCON or siHIF2α and treated with 1μM or 2.5μM statins or 50μM terbinafine +/- 10μM PT2385 (PT) during 5 days relative to cells treated with DMSO. n=3. * p<0.05, ** p<0.01, *** p<0.001. Errors bars depict standard error of the mean.

Supplementary Files

This is a list of supplementary files associated with this preprint. Click to download.

- BMCSupplementaryFigure1.tif
- BMCSupplementaryFigure2.tif
- BMCSupplementarytables2.docx